Proceedings of 10th IOE Graduate Conference
Peer Reviewed
ISSN: 2350-8914 (Online), 2350-8906 (Print)
Year: 2021 Month: October Volume: 10

Design and Simulation of Francis Turbine Runner for Betan Karnali Hydroelectric Project for Original and Reduced Head Condition

Bikki Chhantyal [a], Sulav Parajuli [b], Smarika Tamrakar [b], Hari Bahadur Dura [a]

[a] *Department of Mechanical and Aerospace Engineering, Pulchowk Campus, IOE, Tribhuvan University, Nepal*
[b] *NEA Engineering Company Limited, Nepal*
Corresponding Email: 075msmde006.bikki@pcampus.edu.np

Abstract

Betan Karnali Hydroelectric Project (BKHEP) is expected to experience a variation of the head from 90.82 m to 49.16 m. This difference in the net head of the project occurs if there is an increment in the tailwater level of the project due to the construction of the Karnali Chisapani Multipurpose Project just downstream of BKHEP. The paper focuses on the design and simulation of Francis runner for the existing net head of 90.82 m and determining the possibility of the employing same runner and profile modified runner analyzing hydraulic efficiency of the runner, keeping the outer diameter of the runner unaltered, for the reduced head of 49.16 m. To accomplish the design of Francis runner, a tailored MATLAB program is developed using the Bovet method. The 2D profile of the runner produced is transformed to 3D using ANSYS Bladegen and velocity triangle. Turbogrid is used for meshing and ANSYS CFX is used for simulation. In CFX post-processing, the efficiency and the optimum value of guide vane angle are obtained which is further compared with theoretical values. When simulated under initial design head condition, hydraulic efficiency of 94.19% at guide vane opening of 18.5° which differs by 0.85% and 7.5% with the theoretical values of 95% hydraulic efficiency and 20° guide vane opening respectively. At a reduced head of 49.16 m, using the same runner showed a drastic reduction in hydraulic efficiency to 86.33% at guide vane opening of 31° which is a 7.86% drop in the efficiency. The unsatisfactory performance of the turbine under reduced head conditions indicated the need for variation in the profile of the runner. Numbers of the simulation were carried out varying the beta and lean angle of the blade, one at a time. Optimum efficiency of 90.94% was achieved for lean angle of ±5° at guide vane opening of 30° keeping same outer diameter of the runner.

Keywords

Tail water, Bovet Method, Blade profile, ANSYS, Bladegen, Turbogrid, CFX, Reduced head, Efficiency

1. Introduction

Francis Turbine is a mixed flow type of reaction turbine where water enters the runner of the turbine in the radial direction and leaves the runner in the axial direction. Runner of the Francis Turbine is driven both due to impulse and reaction effect. A total of 995MW planned and proposed hydropower projects in Nepal are planning to use Francis Turbine. The findings from Panta et.al, 2014 showed that almost 75% of the hydropower uses or will use Francis turbines for power generation [1]. This indicates huge scope for Francis turbine manufacturing in Nepal.

The design and manufacturing of the Francis turbine differ from one flow condition to another, which demands tailored design and a special manufacturing process. It is always a challenge to design an efficient Francis runner for two different head and flow rate conditions, and determine the suitability of the runner designed for one condition to use it for the other condition. One such condition prevails in Betan Karnali Hydroelectric Project (BKHEP). Betan Karnali Hydroelectric Project harnesses 688MW of power from the Karnali river [3]. Just downstream of the project, there is another expected hydropower construction of the Karnali Chisapani Multipurpose Project [2]. It is foreseen that the BKHEP experiences variation of the net head from 90.82 m and to 49.16 m due to increment in tailwater level after the construction of the Karnali Chisapani Multipurpose

Project downstream[2,3]. The hydraulic efficiency of a turbine will definitely not be optimum when the runner designed for the initial net head condition is used for reduced head condition.

In this study, analytical and numerical simulations are performed to design a Francis turbine runner blade considering two different net head and flow rate combinations. The main focus of the research is to know the usability of the runner designed for the initial head to be used for reduced head and, change the runner profile and maintain optimum hydraulic efficiency at the reduced net head without changing outer diameter. Various parameters including optimum guide vane openings, flow streamlines, blade loading, and pressure plot in the blade with linear beta distribution for the head of 90.82 m and 49.16 m respectively are examined and analyzed.

Nomenclature

Table 1: Nomenclature

H	Net head, m
Q	Flow rate, m^3/s
g	Acceleration due to gravity, m/s^2
n_0	Dimensionless specific speed
N_0	Rotational speed of runner, rad/s
b_0	Dimensionless guide vane height
l	Dimensionless length
R_{2e}	Specific radius of meridional plane, m
β	Angle of blade, in degrees (°)
v_{2e}	Dimensionless specific volumetric flow rate
i	Hub curve
e	Shroud curve

2. Literature Review

There are several studies about the design of the Francis turbine in the literature. Experimental model test method, Direct method, Inverse method, Bovet, and Conformal mapping method are some of the widely used methods. It is always possible to predict the characteristics of the turbine using model tests in the laboratory. However, time, budget, and prototype constraints contributed to the use of CFD tools for turbine optimization.

The direct method is one of the most important design approaches for Francis turbine design. Here, the designing process begins with specified inlet conditions to determine various dimensions of the runner. Based on the runner dimension, dimensions of other components are calculated [4]. Meanwhile, the Indirect method differs from the direct method as it requires a wide range of input variables which includes available head, discharge, rotational speed, number of blades, camber surface angle/ wrap angle along the leading edge, blade loading distribution, and blade thickness distribution. The indirect method outputs the blade shape that satisfies the inputs, including the required loading distribution, and the associated flow fields [5].

Among all the numerical approaches, one of the most simple and easy-to-use design approaches for Francis turbine runners is the Bovet method which uses empirical equations to obtain parameters of Francis type hydro turbine runner. Bovet formulated the empirical equations based on existing hydraulic turbines where he determined the number of speed factors to obtain the hydraulic profile of a turbine runner's blades [6]. Kocak, E. et al, designed a single blade using the Bovet and Conformal mapping method, performed analytical calculations and numerical simulations on the same. The results of the numerical analysis showed that the Bovet design approach is able to calculate a runner that has an efficiency of 1% difference with respect to committed efficiency [7]. Milos, T. et al presented the advantages of CAD for optimizing the shape of the runner especially in respect of flexibility and computing-time [8].

Ghimire et.al used the Bovet approach and some variations of general techniques to design a Francis turbine for micro-hydro application and manufacturing simplicity. The authors validated the result from numerical simulation with experimental tests at the Turbine testing lab, Kathmandu University. Feasibility studies have suggested that the manufacturing technology available in Nepal is adequate to manufacture the Francis turbines up to 5MW [9]. Bishwakarma, I.B., and Shrestha, R. presented MATLAB software codes for modeling of Francis runner. The authors' model was developed in reference to the runner blade of the Devighat Hydropower Station [10].

Improved Bovet method was used in the research because it is simple, empirical and it tailors to our requirement of keeping outer diameter same as various runner parameters are based on outer diameter. It is widely used because of its ability to accommodate a wide range of variations of the head in designing which pertains to our requirements.

3. Methodology

The required input data of head and flow rate was obtained from NEA Engineering Company. Based on the data, runner parameters were calculated and a meridional plane was obtained which was used as input for ANSYS Bladegen. The 3D model of the blade was constructed by setting the number of blades, Beta angle, and thickness distributions which were then meshed and simulated in TurboGRID and ANSYS CFX respectively to obtain the hydraulic efficiency of the runner. The runner blade profile obtained for design condition of head and flow rate was further simulated under the reduced condition of head to determine the hydraulic efficiency of the runner. Based on the simulation result obtained, the suitability of the same runner blade to be used under the reduced head condition was determined and necessary changes on the runner profile were performed if deemed necessary.

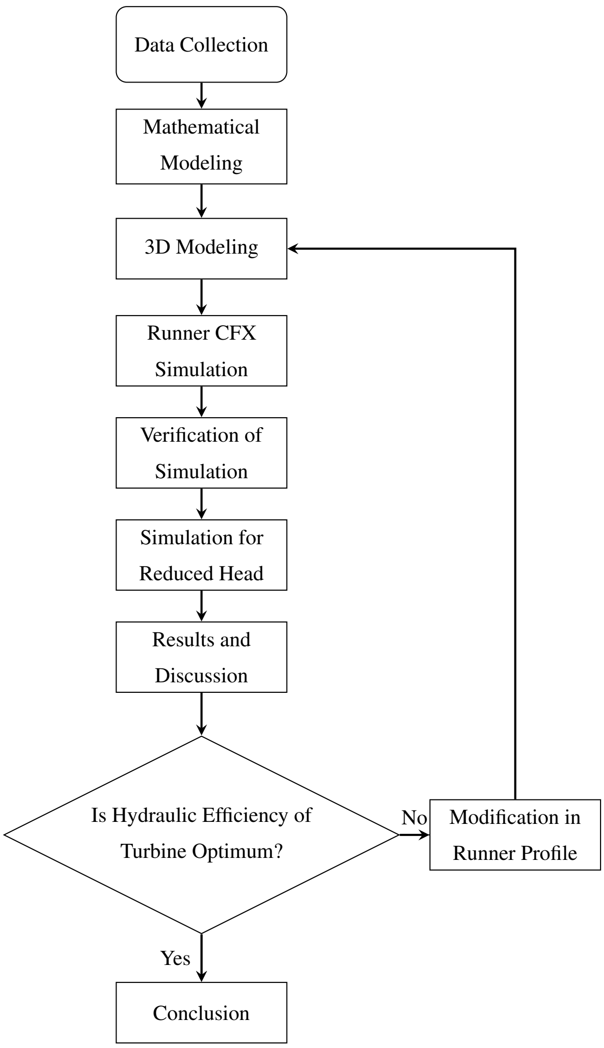

Figure 1: Methodology of the Study

3.1 Data Collection

The information of the net head, volume flow rate, speed of the runner, and a number of blades obtained is tabulated in Table 2.

Table 2: Design Data

	Case 1	Case 2
Net Head	90.82 m	49.16 m
Flow rate	92.37 m^3/s	92.37 m^3/s
Speed	187.5 rpm	187.5 rpm

3.2 Mathematical Modeling

The mathematical modeling was carried out using the Bovet method. 2D meridional profile of the runner including hub, shroud, leading, and trailing edges were obtained using inlet conditions of Case 1. Various parameters required for modeling were obtained using the empirical equation provided by Bovet.

3.2.1 Main Parameters

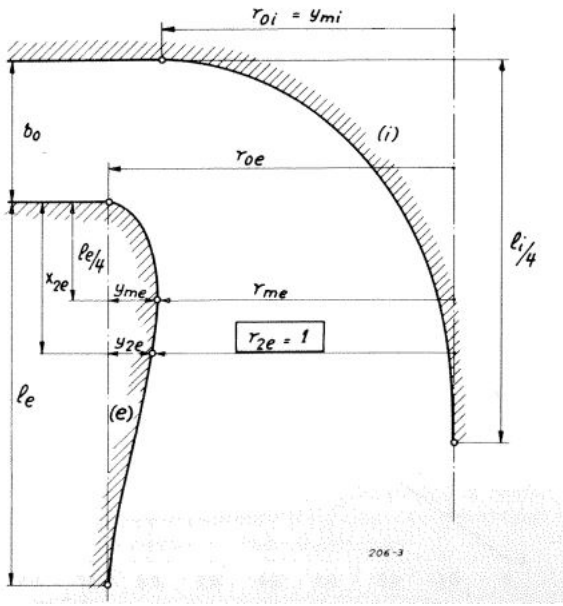

Figure 2: Meridoinal plane of Francis runner

The parameters that completely define the meridional plane were all determined using the non-dimensional specific speed number such that the nominal radius r_{2e} is 1.

All the parameters required for construction of meridional plane depended upon the value of non-dimensional specific speed. The value of non-dimensional specific speed is given by:

$$n_0 = \frac{N_0(\frac{Q}{\pi})^{1/2}}{(2gH)^{3/4}}$$

Based upon the value of n_0 other dimensions were determined using the following formula.

$$b_0 = 0.8(2-n_0)n_0$$

$$r_{oi} = y_{mi} = 0.7 + \frac{0.16}{(n_o+0.08)}$$

$$r_{oe} = r_{li} = \frac{0.493}{n_0^{(2/3)}}(n_0 < 0.275)$$

$$r_{oe} = 1.255 - 0.3n_0(n_0 > 0.275)$$

$$l_i = 3.2 + 3.2(2-n_0)n_0$$

$$l_e = 2.4 - 1.9(2-n_0)n_0$$

$$y_{2e} = r_{oe} - 1$$

$$\frac{y_{2e}}{y_{me}} = 3.08\left(\frac{x_{2e}}{l_i}(1-\frac{x_{2e}}{l_i}\right)^{(3/2)}$$

Where, for Francis runner, the value of x_{2e} is taken 0.5.

The ratio $\frac{y_{2e}}{y_{me}}$ for each value of n_0 was calculated, to determine the value of y_{me}.

$$y_{me} = \frac{y_{2e}}{\frac{y_{2e}}{y_{me}}}$$

To convert these dimensionless values into dimensional values, each parameter calculated above was multiplied with R_{2e} such that;

$$R_{2e} = \left(\frac{\frac{Q}{\pi}}{N_0 \times v_{2e}}\right)^{(1/3)}$$

The value of v_{2e} was taken as 0.27 for the study [4].

3.2.2 Hub and Shroud

Once the value of parameters were determined, coordinates for hub and shroud were generated using assumption that hub and shroud curve are parabolic in nature. $\frac{y_{2e}}{y_{me}} = 3.08\left(\frac{x_{2e}}{l_i}(1-\frac{x_{2e}}{l_i}\right)^{(3/2)}$

The corresponding value of y_{2e} for certain value of x_{2e} in the interval $(0, \frac{l_i}{4})$ for hub and $(0, l_e)$ for shroud gave coordinate combination of hub and shroud curve.

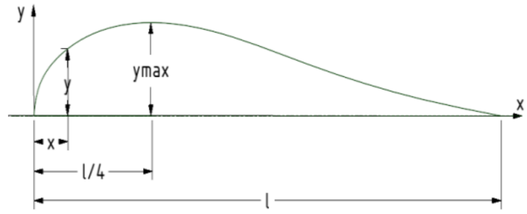

Figure 3: Hub and Shroud Curve Formation

3.2.3 Streamlines

Streamlines are flowlines tangential to instantaneous velocity direction. The coordinates for streamlines were obtained using the linear interpolation technique from shroud to hub.

X- Coordinate for i^{th} Streamline $= \frac{(x_2-x_1)}{(N+1)i} + x_1$

Y- Coordinate for i^{th} Streamline $= \frac{(y_2-y_1)}{(N+1)i} + y_1$

(x_1, y_1) and (x_2, y_2) were the co-ordinates of hub and shroud; N is the number of streamlines.

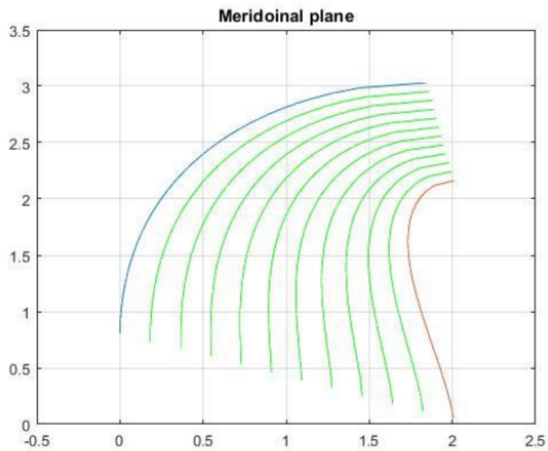

Figure 4: Streamlines on meridoinal plane for Case 1

3.2.4 Leading and Trailing Edge

The leading and trailing edge of the runner is determined using the correlation coefficient provided by Bovet [6]. The intersection of vertical line $y = r_{1i}$ and hub provided one point of leading-edge and the intersection of vertical line $y = r_{2e} \times 1.1$ and shroud provided a second point of trailing edge. Here, 1.1 is the correlation coefficient for shroud and trailing edge for specific speed corresponding to Case 1.

Similarly, the intersection of vertical line $y = r_{2e} \times 0.475$ and hub provided one point of trailing edge and the intersection of vertical line $y = r_{2e}$ and shroud provided the second point of trailing edge, where 0.475 is the correlation coefficient for trailing edge and hub for specific speed corresponding to Case 1. These two points are joined parabolically to make a leading and trailing edge.

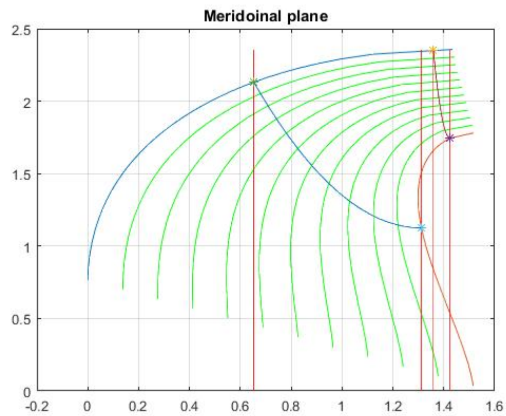

Figure 5: Leading and Trailing edge for Case 1

3.2.5 MATLAB Coding

The mathematical formulations were written in terms of codes in MATLAB script files. Separate functions were prepared for obtaining values of parameters, curve interpolation, a meridional plane with the hub, shroud curve, streamlines, and leading and trailing edge. The net head, volume flow rate, and rotational speed of the runner were taken as the input condition. The 2D meridional plane was created using the tailored MATLAB script file.

4. Modeling and Simulation

4.1 3D Modeling of Francis Runner

The coordinates of the meridional plane were input into ANSYS Bladegen for obtaining a 3D Francis runner. 15 runner blades were created with 5 streamlines in between the hub and a shroud was used to model the runner.

Beta angle was calculated using the following formulae obtained from flow velocity triangle:

$$\cot\beta_1 = \frac{\pi D_{1e} B_1}{Q}\left(\frac{\pi D_{1e} n}{60} - \frac{60 gH}{\pi D_{1e} n}\right)$$

$$\tan\beta_2 = \frac{60Q}{\pi D_{2e} n A_2}$$

D_{1e} and D_{2e} are the diameter at the leading edge and trailing edge respectively for each streamline.

Additionally, constant thickness distribution of 2mm was employed for the modeling.

Figure 6: 3D Geometry of Runner of Case 1

4.2 Meshing

Structured Meshing was done using TurboGRID. The runner was meshed in Turbogrid with the first layer thickness of 1 mm based upon the y^+ value of 1 for the SST $k - \omega$ turbulence model. Mesh independence test was performed by taking efficiency as the parameter of interest with a tolerance of 1% which resulted in mesh with 91440 nodes and 81121 Elements.

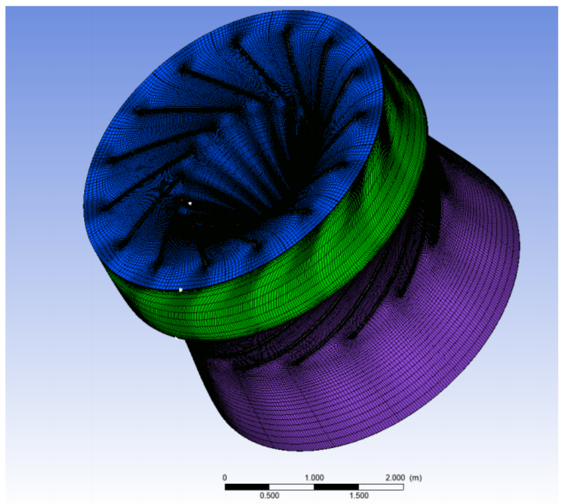

Figure 7: Meshing of Runner of Case 1

4.3 Boundary Condition

Based on the available inputs, mass flow inlet and pressure outlet was selected to specify the inlet and outlet condition of the simulation. The passage of the runner was specified rotating in a clockwise direction. The direction of flow at the inlet was stated using axial, radial, and tangential cylindrical coordinates. The axial directional co-ordinate was specified 0, meaning the flow is completely absent in the axial direction. The radial and tangential direction of the flow was indicated $-\sin\theta$ and $-\cos\theta$, where θ represents the guide vane opening.

Table 3: Boundary Condition

Boundary	Type	Value
Inlet	Mass flow inlet	Mass flow rate: 6128.38 kg/s Cylindrical coordinate:(a,r,t) = $(0, -\sin\theta, -\cos\theta)$
Outlet	Static Pressure outlet	Static pressure: 0 atm
Passage	Rotating	-187.5 RPM (high speed Francis)

4.4 Turbulence Modeling

SST $k-\omega$ turbulence model was chosen for the simulation, as it works well in both free shear flow and near-wall region [11].

Kinematic eddy viscosity:

$$\nu_\tau = \frac{a_1 k}{max(a_1\omega, SF_2)}$$ Turbulence kinetic energy:

$$\frac{dk}{dt} + U_j\frac{dk}{dx_j} = P_k - \beta_k\omega + \frac{d}{dx_j}[(\nu + \alpha_k\nu_\tau)\frac{dk}{dx_j}]$$

Specific dissipation rate:

$$\frac{d\omega}{dt} + U_j\frac{d\omega}{dx_j} = \alpha_k S^2 - \beta\omega^2 + \frac{d}{dx_j}[(\nu + \alpha_k\nu_\tau)\frac{dk}{dx_j}] + 2(1-F_1)\alpha_{\omega^2}\frac{1}{\omega}\frac{dk}{dx_i}\frac{d\omega}{dx_i}$$

4.5 Post Processing

The flow streamlines, blade loading, and pressure in the blade for the design condition are studied rather than efficiency to verify the compliance with the physics of the fluid flow.

4.5.1 Flow Streamlines

The streamline in the single passage is transformed into full blade rotation to obtain complete flow streamlines. From the streamlines, we can observe more or less axial flow with respect to the stationary frame of reference, at the outlet which confirms the initial design condition.

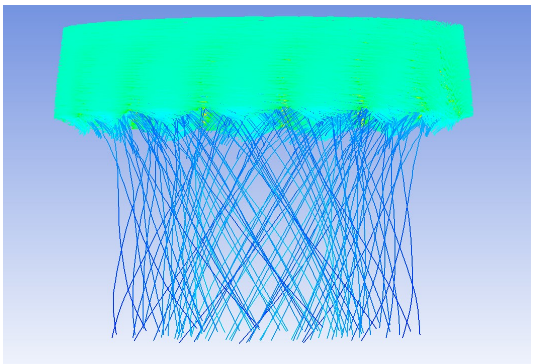

Figure 8: Flow Streamlines for case 1

4.5.2 Blade Loading

The pressure distribution in the pressure side and the suction side along the streamline is called blade loading.

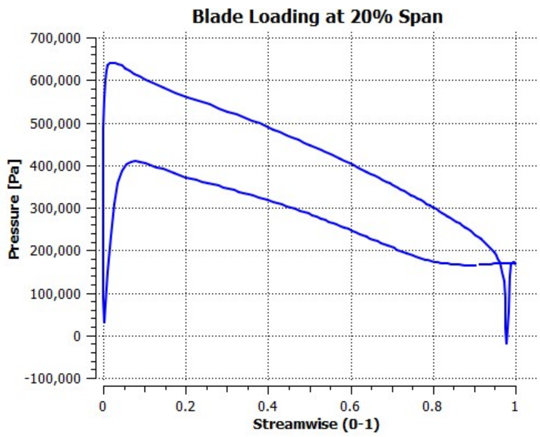

Figure 9: Blade Loading at 20% span for Case 1

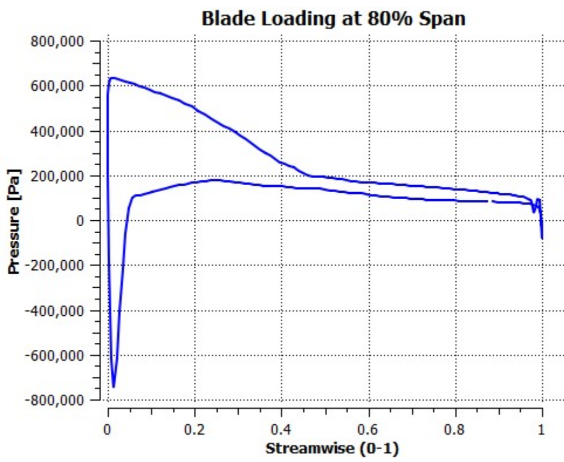

Figure 10: Blade Loading at 80% span for Case 1

From simulation results, it is evident that the pressure is high on the pressure side and low on the suction side. There is a huge difference in pressure in the leading-edge region due to the formation of the stagnation region at the suction side. Similarly, there is negative differential pressure at the trailing edge side of a very small region due to little vortices and backflow. In the case of the 80% span length region, the intensity of the vortex is rather negligible. Furthermore, the pressure difference is high in the 80% span. This indicates that the rotation is created by impact rather than a lift when the span is increased.

4.5.3 Pressure in the Blade (Contour)

The pressure difference in the blade creates the lift whose moment about the axis creates the rotation of the blade.

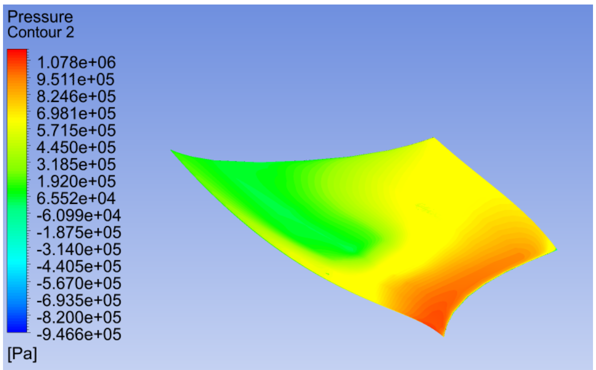

Figure 11: Pressure Contour on pressure side -Case 1

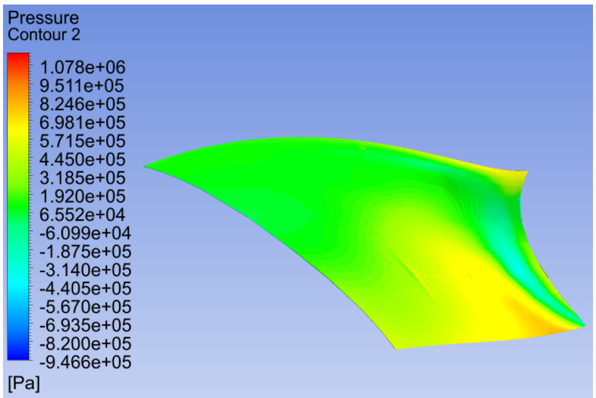

Figure 12: Pressure Contour on suction side -Case 1

Figure 11 and Figure 12 show the pressure distribution on the pressure and suction side of the blade. The pressure is abrupt but linearly distributed along the span in the pressure side. However, spanwise pressure variation is small in the case of the suction side. There is high negative pressure near the leading edge and, region of small negative pressure near the trailing edge in the suction side which is due to the formation of vortices.

5. Results and Discussion

5.1 Results

5.1.1 Case 1: Design Flow Condition

The simulation run is carried out for different conditions with a target residual value of 0.0001. Flow streamlines, blade loading at 20%, and 80% blade span, and fluid pressure on the blade are plotted for each of the conditions. Efficiency corresponding to the guide vane openings required on each case for respective head recovery is noted under these conditions. The value of guide vane opening angle is varied in each simulation run to obtain the head recovery of 90.82 m for Case 1 and corresponding efficiency is noted. For this purpose, the theoretical value of the guide vane opening angle is determined using a velocity triangle. This theoretical value of guide vane opening will serve as starting opening angle to determine the optimum opening required for associated head recovery. The change in guide vane opening angle to recover head is suggested by Kristine [12]. A similar procedure has have been followed for Case 2 as well.

Table 4: Simulation Result for Case 1

Guidevane opening (°)	Flow rate (m^3/s)	Head (m)	Efficiency (%)
20	92.37	82.38	94.15
19	92.37	88.11	94.12
18	92.37	94.65	93.99
18.5	92.37	90.21	94.19

Table 5: Comparision of Theoretical and Simulation Results

Parameter	Calculation	Simulation	Difference
Flow rate	92.37 m^3/s	92.37 m^3/s	0.00%
Head	90.82 m	90.21 m	0.67%
Efficiency	95%	94.19%	0.85%
GV angle	20°	18.5°	7.5%

There is no significant difference between theoretical and simulated results. Hence, the simulation can be verified.

5.1.2 Case II: Reduced Head Condition

The simulation result when the runner blade designed for Case 1 is used to operate under Case 2, is presented in Table 6. There is a significant change in the efficiency of the turbine when used under reduced head conditions. The efficiency of 94.19% at head 90.82 m is reduced to 86.33% at the head of 49.16 m. This indicates a drop of about 9% in hydraulic efficiency of the turbine considering that the guide vane can be opened up to 31°. With such a drastic alteration in the hydraulic efficiency of the turbine, it is evident that the runner needs some modification to improve its efficiency. As the outlet diameter of the runner is unchanged at all times, the only parameter we can vary to get optimum results is the blade profile. This modification is discussed under Section 5.1.3.

Table 6: Simulation Result for Case 2- Unmodified Profile

Guidevane opening (°)	Flow rate (m^3/s)	Head (m)	Efficiency (%)
20	92.37	82.38	84.17
25	92.37	61.61	85.93
30	92.37	50.27	86.05
31	92.37	48.41	86.33

5.1.3 Modification of Runner Profile

In order to perform modification in the profile of the runner, the distribution of beta angle and lean angle of the blade is varied. The result of hydraulic efficiency obtained by varying the profile of the runner is tabulated below.

Table 7: Simulation Result for Case 2- Modified Profile

Condition	Guidevane Opening (°)	Efficiency (%)
Linear beta distribution	31	86.33
Concave 10 %	31	87.92
Concave 20 %	32.5	87.69
Convex 10%	30	87.37
Convex 20%	29	86.06
Sinusoidal (5% up, down)	32.5	85.25
Lean angle -10 °	30	88.25
Lean angle -5 °	30	89.95
Lean angle 5 °	30	90.94
Lean angle 10 °	30	90.75

A new hydraulic efficiency of 90.75% is obtained for the net head of 49.16 m. With the modification of profile, a gain in 4.42% of hydraulic efficiency is observed at a lean angle of +5°from the original profile.

5.2 Discussion

There is no significant variation in efficiency although the variation in head is about 50%. This can be explained on the basis of different points.

5.2.1 Non dimensional speed number

The value of n_0 governs the shape of the meridional plane and hence the geometry of runner.

Case 1: $n_0 = 0.39$

Case 2: $n_0 = 0.61$

Bovet suggest that the variation in meridional plane is negligible when $n_0 = 0.4$ and $n_0 = 0.6$.

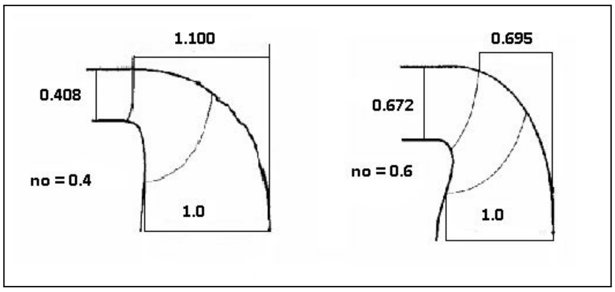

Figure 13: Meridoinal plane and Non-dimensional speed

As the meridional profile of the runner is similar in both cases, no significant change in the geometry of the runner takes place. This in turn causes similar hydraulic performance of runners in both cases.

5.2.2 Specific Speed

The specific speed of the turbine is an important parameter to determine the design of the runner. The specific speed before and after head reduction is compared.

Case 1: 191.38 rpm

Case 2: 303 rpm

Both are in the high-speed Francis turbine region of 50-300rpm. Hence, no significant variation in the hydraulic efficiency of the runner exists when the profile is modified.

6. Conclusions and Recommendations

The simulation carried out for a net head of 90.82 m at flow rate 92.37 m^3/s and speed 187.5 rpm resulted in hydraulic efficiency of 94.19% at guide vane opening angle of 18.5°. When the same runner is used at a reduced net head of 49.16 m with the same flow rate of 92.37 m^3/s and speed of 187.5 rpm, hydraulic efficiency of 86.33% is obtained at a guide vane opening angle of 31°. Further simulations carried out by varying blade profiles resulted in a gain in hydraulic efficiency. The hydraulic efficiency of 90.94 % was achieved for lean angle +5°at guide vane opening of 30°. Thus, the replacement runner with the lean angle +5°having an equal diameter as previous can be done with $<$ 5% decrements in the efficiency.

Certain recommendations to further improve the simulation result are as follows:

1. Experimental verification can be performed.
2. Difference interval is kept 5°due to computational constraints, reducing the difference is recommended to obtain better results.
3. Combination of lean and beta distribution, which was outside the scope of our research, may also provide better results.
4. Optimization can be performed using algorithms.
5. Whole turbine can be simulated instead of runner passage only.

References

[1] Panta, S., Lamsal, M., Thapa, B. (2014). Prediction of Turbine Needed For Future Hydropower Projects In Nepal. Hydro Nepal: Journal of Water, Energy and Environment, 14, 23-26.

[2] Raina, D.N., Acharya, M.P., Bhattarai, L. (2017). Review of Karnali (Chisapani) Multipurpose Project (10,800 MW) Feasibility Studies Carried out in 1989.

[3] NEA Engineering Company Limited, Betan Karnali Hydroelectric Project, Retrieved form: http://neaec.com.np/en/projects/detailed-engineering-study/betan

[4] Kaewnai, S., Wongwises , S. (2011). Improvement of the Runner Design of Francis Turbine using Computational Fluid Dynamics. American Journal of Engineering and Applied Sciences , 540-547.

[5] Open-Source Implementation and Validation of a3D Inverse Design Method for Francis TurbineRunners by Sebastian Leguizam ´ on * andFran ´ c¸oisAvellanOrcID

[6] Bovet T. Contribution to the study of Francis –Turbine Runner Design. Lausanne; 1963

[7] Kocak, E., Karaaslan, S., Yucel, N., Arundas¸, F.(2017). A Numerical Case Study: Bovet Approach toDesign a Francis Turbine Runner. Energy Procedia,111, 885-894.

[8] MILOS, T. (2004). CAD TECHNIQUE USED TOOPTIMIZE THE FRANCIS RUNNER DESIGN.

[9] Ghimire, A., Dahal, D.R., Pokharel, N., Chitrakar,S., Thapa, B. (2019). Opportunities and Challenges ofintroducing Francis Turbine in Nepalese MicroHydropower Projects.

[10] Biswakarma, I.B., Shrestha, R. (2018).Mathematical Modeling for the Design of FrancisRunner

[11] Hellsten, A. (1998). Some improvements inMenter's k-omega SST turbulence model. In 29thAIAA, Fluid Dynamics Conference (p. 2554).

[12] Gjøsæter, K. (2011). Hydraulic design of Francisturbine exposed to sediment erosion (Master's thesis,Institutt for energi-og prosessteknikk)